



# Effects of Two-Way Turbulence Interaction on the Evaporating Fuel Sprays

H. Khaleghi<sup>†</sup>, M. Ahmadi and H. Farani Sani

*Tarbiat Modares University, Tehran, 14115-111, Iran*

<sup>†</sup>*Corresponding Author Email: khaleghi@modares.ac.ir*

(Received June 21, 2018; accepted January 14, 2019)

## ABSTRACT

This article discusses the importance of using different turbulence modulation models in simulation of evaporating sprays. An in-house CFD code has been modified to take into account the effect of considering turbulence modulation by standard or consistent models. These models may predict an augmentation (consistent model) or a reduction (standard model) in the turbulence kinetic energy of continuous phase. Calculations are done in a Eulerian-Lagrangian framework and the effect of injected droplets on turbulent kinetic energy and its rate of dissipation is included in the equations of the continuous phase. Results are shown to be valid by comparing them to Sandia spray A configuration experimental data. Results show that considering the effect of existing droplets in a turbulent combustion chamber can play a major role in having a more accurate CFD simulation. These models can alter the velocity field drastically when droplets are injected into the chamber with a high velocity. As a result, spray characteristics such as evaporation rate is also altered. It can be concluded that modulation models should be used in the simulation of evaporating sprays in order to attain more accurate and realistic results.

**Keywords:** Turbulence modulation; Turbulent dispersion; Evaporation rate; Velocity profile alternation.

## NOMENCLATURE

$C_d$	drag force coefficient	$t$	temporal coordinate
$C_p$	specific heat in constant pressure	$u$	velocity vector
$D$	diameter	$V$	computational cell volume
$f$	fuel vapor mass fraction	$x$	spatial coordinate
$h$	total energy	$\Gamma$	diffusion coefficient
$k$	turbulence kinetic energy	$\theta$	mixture void fraction
$m$	mass	$\mu$	viscosity
$p$	pressure	$\rho$	density
$Re$	Reynolds number	$\varepsilon$	turbulent dissipation rate
$S$	source term	$\alpha$	droplet volume fraction
$T$	temperature		

## 1. INTRODUCTION

The application of turbulent flows laden with particles or droplets is in many areas of interest. A few examples are sandstorms, spray drying processes, and combustion of fuels, which the mixing is mainly controlled by the turbulence of the carrier phase. Because of the momentum, heat, and mass transfer between the droplets and the continuous phase, there will be a great difference in the characteristics of carrier flow in comparison to clean flow (single-phase flow) and on the other hand, turbulence can alter the trajectory, heat, and mass

transfer properties of the dispersed phase to a high extent. Previous studies about the alternation of turbulence by particles or droplets have shown that the presence of the dispersed phase in a flow can either augment or attenuate the continuous phase turbulent kinetic energy and its rate of dissipation. Turbulence modulation is the title usually referred to this phenomenon as in [Elghobashi and Abou-Arab \(1983\)](#).

Many researchers have studied this interaction by theoretical analysis, experimental measurements or numerical modeling and a wide range of results have been reported by them [Luo et al. \(2016\)](#). Although

there are numerous studies in the literature, the fundamental mechanism responsible for this modification is still ambiguous, Crowe (2000).

Gore & Crowe (1989), Hetsroni (1989) summarized the experimental data until then and suggested the criteria for the augmentation or suppression of turbulence. Gore and Crowe (1989) found that the  $d_p/l_e$  parameter is a criterion that when it is smaller than 0.1, the existence of dispersed phase results in a decrease in turbulence level (small droplets reduce turbulence kinetic energy of the flow). And when this parameter is greater than 0.1, it causes an increase in the turbulence level (bigger droplets enhance the turbulent kinetic energy). Hetsroni (1989) found another criterion based on particle Reynolds number. He proposes that droplets, which have high Reynolds number, increase turbulence and those with a low Reynolds number, attenuate it. Other researchers Paris and Eaton (2001) also suggested that mass loading does also influence the turbulence at low particle Reynolds number. Continuing on this path, Ferranate and Elghobashi (2003) found that the ratio of particle response time to the Kolmogorov time scale can predict the increase, decrease, or no net change in turbulent kinetic energy.

Balachandar and Eaton (2010) claimed that there are three major possible scenarios concerning the turbulence modulation. They classified them as:

- 1- An increase of dissipation rate by droplets with extracting kinetic energy from eddies.
- 2- Transferring of energy from dispersed phase to the continuous phase e.g. if the droplets have higher velocities in comparison to gas phase because of initial conditions.
- 3- Wake formation behind the large droplets.

In a more recent research, Luo *et al.* (2016) classified turbulence modulation by finding a novel dimensionless parameter using dimensional analysis of the momentum equation for turbulent flows laden with particles combined with the Buckingham  $\Pi$  theory. They validated their proposed parameter by a set of 238 experimental data. They also suggested an empirical formula to estimate the turbulence modification, quantitatively.

As stated by Crowe (2005) many models have been developed but none of them are capable of considering all of the above-mentioned factors in CFD simulations. In general, researchers emphasize on the fact that fundamental physics of the phenomenon is not quite known yet and there should be more experimental and numerical studies on this area to shed more light on this kind of problems.

The focus of this work is on the numerical investigation of turbulent modification in evaporating sprays. Most of the numerical studies in the literature (Ebrahimi and Crapper, 2017; Meyer, 2012; Alvandifar *et al.*, 2011; Lain and Sommerfeld, 2008) just considered the solid particles in gaseous flows, which means they did not consider heat and mass transfer between the two phases. Moreover, the degree of importance of considering these models in CFD simulation of evaporating fuel sprays has not

been investigated yet.

In CFD modeling of this phenomenon, the general trend is to add source terms in the formulation of both turbulent kinetic energy and turbulent dissipation rate of the single-phase flow to consider the existence of the second phase. There are various models proposed for these source terms and they are dependent on the model of turbulence used for closing the momentum equations of the fluid. Most of them have chosen the k- $\epsilon$  model but there are also a few models developed for the k- $\omega$  model (Lain and Sommerfeld, 2008; Lun, 2000). The above-mentioned source terms usually are classified into two categories: standard and consistent approaches. The formulation of these methods, based on the k- $\epsilon$  model is provided in the next sections.

## 2. GOVERNING EQUATIONS

The selected approach for solving two-phase flow in evaporating fuel spray is Lagrangian-Eulerian which solves the continuous phase (air-fuel vapor mixture) based on Eulerian equations (source terms included for considering the second phase) and uses Lagrangian equations for dispersed phase (fuel droplets). In this approach, a finite number of parcels, which each one of them is representing a number of droplets with the same properties, forms the spray. In the following sections, the equations for both phases will be provided in detail.

### 2.1 Eulerian Phase Equations

The differential equations governing the conservation of mass, momentum, energy, Turbulent kinetic energy, turbulent dissipation rate, and fuel vapor mass fraction form the theoretical basis for this kind of problems. By assuming that the in-cylinder processes can be adequately described by their statistically averaged properties, equations are used in the ensemble-averaged form. It should be noted that the averaging used here is that of density-weighted or Favre averaging that can be found in Bilger (1975). The domain of the combustion chamber is divided into the cylinder and piston bowl regions (Fig. 1(a)).

The cylinder zone is called Expanding/Contracting region in which the volume of cells changes with time. The second region is called translating region, which only translates in Z direction with a constant velocity and meshes in this region are driven in orthogonal and in a curvilinear coordinate system.

The general transport equation takes the following shape in both regions:

$$\frac{1}{\delta V} \frac{\partial (\rho \delta V \phi \theta)}{\partial t} + \nabla \cdot (\rho \phi u_{rel} \theta) = \nabla \cdot (\mathcal{A}_\phi \nabla \phi) + S_\phi + S_{\phi,d} \quad (1)$$

Where  $\delta V$  is a computational cell volume,  $\theta$  is the void fraction of the cell, which is the portion of the cell which is filled with gas mixture.  $\rho$  is the mixture density,  $\phi$  is the transported variable,  $u_{rel} = u - u_{grid}$  is the vector of relative velocity,  $S_\phi$  is the

source term, and  $S_{\phi,d}$  is the source term because of the droplet phase interactions with the gas phase. Various parameters which can be substituted for  $\phi$ ,  $\Gamma$ , and  $S$  are as stated in Table 1.

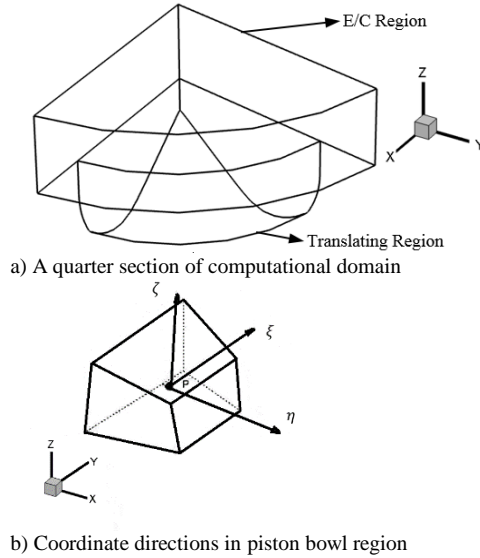


**Fig.1. Computational domain regions and coordinate directions.**

A major difference between these two regions (between the piston surface and the cylinder head) is that computational domain is moving with a local absolute velocity of  $u_{grid}$  (depends on engine's speed) in the E/C region which results in volume change with time but there are no such changes in the translating region.

The difference between single phase flow and the droplet-laden one is in the term  $S_{\phi,d}$ , which will be introduced in the next section.

**Table 1 Variables for general transport equation**

Variable	$\phi$	$\Gamma_\phi$	$S_\phi$
Mass	1	0	0
Velocity	$u$	$\mu_{eff}$	$\theta \partial p / (\partial x_i)$
Energy	$h$	$\mu_{eff} / \sigma_h$	0
Turbulent energy	$k$	$\mu_{eff} / \sigma_k$	$P_k - \varepsilon$
Eddy Dissipation Rate	$\varepsilon$	$\mu_{eff} / \sigma_\varepsilon$	$C_{1\varepsilon}(\varepsilon/k)(P_k) - C_{2\varepsilon}(\varepsilon^2/k)$
Fuel Vapor Mass Fraction	$f$	$D$	0

## 2.2 Lagrangian Phase Equations

The droplet momentum and trajectory equations adopted in this work are as follows:

$$\frac{du_{i,d}}{dt} = K_d (u_i - u_{i,d}) - \frac{1}{\rho_d} \left( \frac{dp}{dx_i} \right) \quad (2)$$

$$K_d = \frac{3}{4} C_d \left( \frac{\rho_g}{\rho_d} \right) \frac{1}{D_d} |u_i - u_{i,d}|$$

$$\frac{dx_{i,d}}{dt} = u_{i,d} \quad (3)$$

Two important forces considered in Eq. (2) are drag and pressure difference forces. In the Eqs. (2,3),  $x_{i,d}$  represents the spatial coordinate and  $t$  represents temporal coordinate,  $u_{i,d}$  is droplet velocity,  $\rho_g, \rho_d$  are the gas and droplet density, respectively,  $p$  is the pressure,  $C_d$  is the drag coefficient, and  $D_d$  is the droplet diameter.

According to [Isbin \(1970\)](#) studies, the Reynolds number is used to evaluate the drag coefficient  $C_d$ . Thus:

$$C_d = 0.44 \quad Re_d > 1000$$

$$C_d = \left( 24 + 3.6 Re_d^{0.687} \right) / Re_d \quad Re_d \leq 1000 \quad (4)$$

In which particle Reynolds number is defined as  $Re_d = \rho_g |u_g - u_d| D_d / \mu_g$ .

Droplet temperature and mass histories are calculated from [Borman and Johnson \(1962\)](#) equations:

$$\frac{d(m C_p T)_d}{dt} = -\pi D_d K (T_g - T_d) \left\{ z / (e^z - 1) \right\} Nu + Q \frac{dm_d}{dt} \quad (5)$$

$$\frac{dm_d}{dt} = -\frac{\pi D_d D P_t \ln \left\{ (P_t - P_{v,\infty}) / (P_t - P_{v,s}) \right\} Sh}{RT_m} \quad (6)$$

In Eq. (5),  $C_p$  is the specific heat at constant pressure,  $K$  is the thermal conductivity and  $Q$  is the latent heat of evaporation. In Eq. (6),  $D$  is the diffusivity,  $P_t$  is the total pressure,  $P_{v,\infty}$  is the vapor pressure far from the droplet surface,  $P_{v,s}$  is the vapor pressure at the droplet surface,  $R$  is the global gas constant, and  $T$  is the temperature. The subscript  $m$  denotes a mean of gas and droplet values.

$z$  in Eq. (5) is the argument of a function which corrects the heat transfer coefficient when the mass transfer is simultaneously taking place and is defined as:

$$z = -\frac{C_{pv} \frac{dm_d}{dt}}{\pi D_d K Nu} \quad (7)$$

Where  $C_{pv}$  is the fuel vapor specific heat. The Nusselt number,  $Nu$  and Sherwood  $Sh$  are evaluated from the following expressions introduced in [Ranz and Marshall \(1952\)](#):

$$Nu = 2.0 + 0.6 Re_d^{0.5} Pr^{1/3} \quad (8)$$

$$Sh = 2.0 + 0.6 Re_d^{0.5} Sc^{1/3} \quad (9)$$

Where  $Sc = \frac{\mu_g}{\rho_g D}$ ,  $Pr = \frac{C_{pg} \mu_g}{K}$ , and  $\mu_g$  is the gas

viscosity.

The source terms for considering the coupling between the droplets and the continuous phase are defined as:

$$S_{m,d} = -\frac{\pi \rho_d}{6 \delta t} \sum_k N_{d,k} \left[ \left( D_{d,k}^{n+1} \right)^3 - \left( D_{d,k}^n \right)^3 \right] \quad (10)$$

$$S_{u,d} = -\frac{\pi \rho_d}{6 \delta t} \sum_k N_{d,k} \left[ \left( D_{d,k}^{n+1} \right)^3 U_{d,k}^{n+1} - \left( D_{d,k}^n \right)^3 U_{d,k}^n \right] \quad (11)$$

$$S_{h,d} = -\frac{\pi \rho_d}{6 \delta t} \sum_k N_{d,k} \left[ \left( D_{d,k}^{n+1} \right)^3 \left( C_p T_{n,k} \right)^{n+1} - \left( D_{d,k}^n \right)^3 \left( C_p T_{n,k} \right)^n \right] \quad (12)$$

In the Eqs. (10, 11, 12), the summations are over all parcels, and  $N_{d,k}$  is the number of droplets in the  $k_{th}$  parcel. The superscripts  $n$  and  $n + 1$  refer to values at two different times separated by droplet integration time  $\delta t$  that is controlled by a couple of time scales in order to capture crossing trajectory effect. [Shuen \*et al.\* \(1983\)](#) proposed that the integration time of droplets should be picked a minimum value between two time scales.

$$\tau_{integral} = \min(\tau_e, \tau_{tr}) \quad (13)$$

The first time scale is the eddy lifetime that is defined as:

$$\tau_e = \frac{l_e}{\sqrt{2k/3}} \quad l_e = \frac{C_\mu^{3/4} k^{3/2}}{\varepsilon} \quad (14)$$

Where  $l_e$  is the characteristic length scale of eddy size, and  $C_\mu$  is the empirical constant of the k-ε model.

The second one is the time for a droplet to cross the eddy which is trapped in:

$$\tau_{tr} = \tau_d \ln \left( 1 - \frac{l_e}{\tau_d |u_g - u_d|} \right) \quad (15)$$

Because the focus of this article is on the source terms for  $k$  and  $\varepsilon$  equations, they will be provided in a separated section with more details.

### 2.3 Spray Sub-Models

Two active forces on droplets are aerodynamic forces and forces due to surface tension. The condition, which the droplet goes under certain deformation, is when the aerodynamic forces overcome surface tension forces. One of the models which is very famous for modeling the breakup process is [Reitz and Diwakar \(1986\)](#) model. This model considers two modes of breakup: Bag breakup for low Weber numbers and stripping breakup for

higher Weber numbers. The threshold for the start of breakup is  $We_c = 6$  which this model decides which mode of the breakup will happen for the parcel of droplets.

Spray at the start of injection is assumed to be fully atomized. The diameter distribution at nozzle exit is calculated by Rosin-Rammler function.

Because of the type of closure for turbulence equations, the exact value of the continuous phase velocity at the droplet position is not available. There are models in the literature for calculating the fluctuation velocity of gas phase which needs to be added to mean velocities, in order to incorporate a better estimation of the continuous phase velocity at droplet position. The random walk model [Yuu \*et al.\* \(1978\)](#) have been chosen in this paper. But it is an open question that whether this model is applicable under high turbulence intensity conditions in engines with high swirl ratio and special arrangements and shapes of piston bowl or not.

This model generates a random number from a normal distribution with a zero mean and unit standard deviation and then multiplies it in the square root of turbulent kinetic energy:

$$u' = \Gamma \sqrt{\frac{2k}{3}} \quad (16)$$

Here  $u'$  is the fluctuation velocity, which will be added to the time averaged velocity,  $\Gamma$  is a random number and  $k$  is the turbulent kinetic energy of gas mixture in droplet's computational cell.

### 2.3 Turbulence Modulation

There are various models for source terms of turbulent kinetic energy and turbulent dissipation energy proposed in the literature. They are usually categorized into standard and consistent models.

#### Standard Approach

In this type of methods, the modeling process starts from momentum equation and then multiplied by the velocity, then Reynold's averaging is applied; by subtracting the mean kinetic energy from this equation, the turbulent kinetic energy due to the existence of droplets is obtained. More details can be found in [Chen and Wood \(1985\)](#). In cases, where only drag force, is important, the following terms can be obtained for turbulent kinetic energy and rate of dissipation equations:

$$S_{k,d} = \frac{\alpha}{\tau_d} \left( \overline{u'_i u'_{di}} - \overline{u'_i u'_i} \right) \quad \overline{u'_i u'_i} = 2k \quad (17)$$

$$S_{\varepsilon,d} = \frac{\alpha}{\tau_d} \left( \overline{v \frac{\partial u'_i}{\partial x_j} \left( \frac{\partial u'_{di}}{\partial x_j} - \frac{\partial u'_i}{\partial x_j} \right)} \right) \quad (18)$$

Where  $\alpha$  is the droplet volume fraction defined as the mass of the droplets per unit volume and

$$\tau_d = \frac{4\rho_d D_p^2}{3\mu_g Re_d C_d}$$

This kind of models are often referred as being

dissipative because they consider that droplets are accelerated by fluid and thus  $u'_{di}$  is smaller than  $u'_i$ , so this quantity is always negative and acts like a sink in turbulent kinetic energy equation according to Elghobashi (1994). Researchers have tried to propose models for the unknown term ( $\overline{u'_i u'_{di}}$ ).

Lightstone and Hodgson (2004) derived an analytical solution for unknown correlation ( $\overline{u'_i u'_{pi}}$ ) by considering the crossing trajectory effect, as:

$$\overline{u'_i u'_{di}} = 2k \frac{\tau^*}{\tau^* + \tau_d} \frac{1}{\tau^*} = \frac{|u_i - u_{pi}|}{L_i} + \frac{1}{\tau_{L_i}}$$

$$L_i = 2\tau_{L_i} \sqrt{2k/3} \quad \tau_{L_i} = 0.135 \frac{k}{\varepsilon} \quad (19)$$

Where  $L_i$  and  $\tau_{L_i}$  are the Lagrangian length and time scales, respectively. In a similar fashion, the source term for ( $\varepsilon$ ) equation, is obtained by multiplying the source term of kinetic energy by ( $\varepsilon/k$ ) and a constant:

$$S_{\varepsilon,p} = C_{\varepsilon_3} \frac{\varepsilon}{k} S_{k,p} \quad (20)$$

### Consistent Approach

Crowe (2000) proposed that by starting from mechanical energy equation of fluid and performing averaging procedures, one can obtain an equation for turbulent kinetic energy which has two terms for considering droplets; one term is called the generation of energy by droplets and the second term is redistribution term. He claimed that the second term is negligible in dilute flows. By considering only, the drag force, the source term will be as:

$$S_{k,p} = \frac{\alpha}{\tau_d} \left( \overline{|u_i - u'_{di}|^2} + \overline{u'_{di} u'_{di}} - \overline{u'_i u'_{di}} \right) \approx \frac{\alpha}{\tau_d} \left( \overline{|u_i - u'_{di}|^2} \right) \quad (21)$$

As can be seen in the equation, this term is always positive and this model can only predict an increase of kinetic energy because of the existence of droplets. The source term for dissipation rate is similar to the previous method and the constant value ( $C_{\varepsilon_3}$ ) has been proposed to be 1.8 by Lain and Sommerfeld (2003).

### 2.4 Numerical Details

Our CFD code solves all the equations presented in the previous sections by finite volume method. The implicit non-iterative Engine PISO algorithm of Ahmadi-Befruji *et al.* (1990) has been applied to resolve the pressure-velocity coupling. The sequence of computations at each time step is as follows:

- Prediction of the velocity field using given pressure and boundary conditions.
- First correction of the velocity field, which satisfies the continuity equation.
- Second correction of velocity field which is similar to the first correction and applies the velocity and pressure fields of the first step

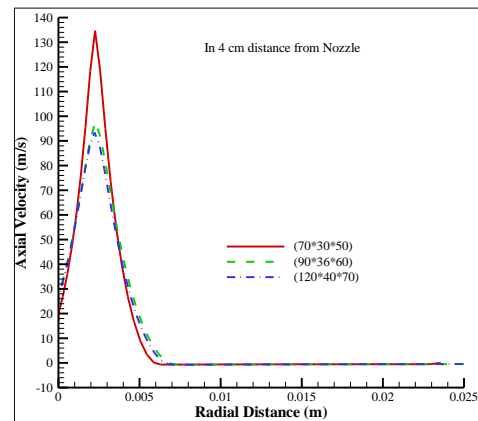
It should be mentioned that before the prediction

stage and after both correction steps, the droplets' calculations are done.

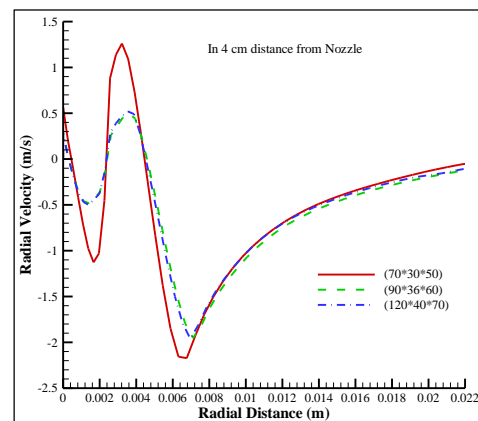
After two steps of correction, the evaporated fuel mass fraction, gas phase energy equation and transport equations of  $k$  and  $\varepsilon$  are solved and then it moves forward to the next time step. It is worth mentioning that there is a mechanism in this code responsible for the correction of  $k$  and  $\varepsilon$  after the convergence of all equations in each time step for each computational cell. Interested readers can find the details of this method in (Khaleghi *et al.*, 2008; Watkins and Khaleghi 1990).

### 3. Results and Discussion

This section starts with the mesh independent results of the code; then numerical results are validated by comparing the results with the SANDIA experimental data. The result section consists of the performance of different modulation models in different chambers and operation conditions to assess their level of predictability.



a) Axial velocity diagram in a radial plane 4 cm from nozzle



b) Radial velocity diagram in a radial plane 4 cm from nozzle

**Fig. 2. Calculated velocity components of continuous phase using three different meshes.**

### 3.1 Mesh Independent Results

For achieving mesh independent results, flow field parameters and spray tip penetration were studied. The numbers which are written in parenthesis in Figs. 2 and 3 show the number of computational cells in axial, circumferential, and radial directions, respectively for three different meshes. Figure 2(a) is the continuous phase's axial velocity ( $w$ ) diagram versus radial direction, in a distance from the nozzle and Fig. 2(b) is the radial velocity ( $v$ ). Also, Fig. 3 is the calculated spray tip penetration during injection time using three different computational meshes. Both of these figures certify that choosing the second mesh can provide us with satisfactory and accurate results.

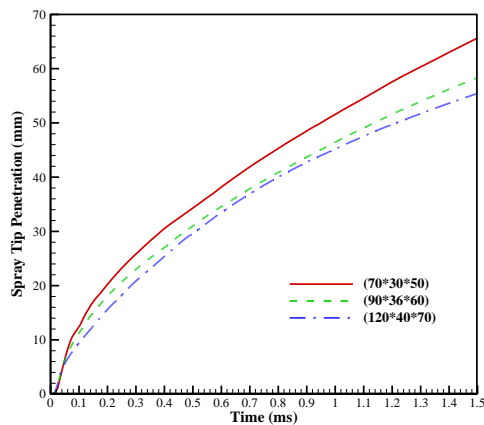


Fig. 3. Calculated spray tip penetration using three different meshes.

Furthermore, comparing the velocity vector plot and mixture temperature contour in Fig. 4 between two meshes can provide another vision concerning mesh independent results.

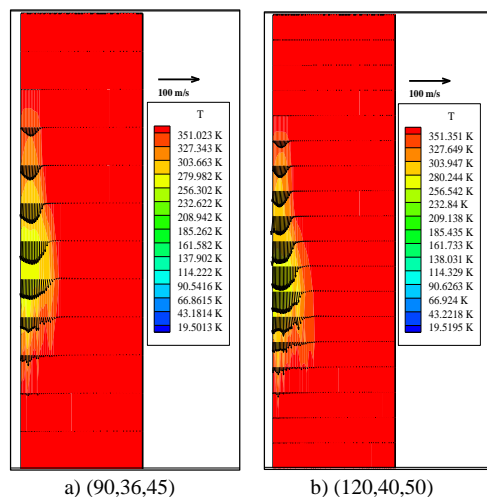


Fig. 4. Temperature contour and vector plot in injection plane using different meshes.

Figure 4 is showing a good agreement between the results of meshes in calculating temperature and velocity parameters in the combustion chamber.

### 3.2 Validation

Results of the experimental data are extracted from SANDIA laboratory known as spray A configuration which is the injection of n-Heptane fuel into a constant volume chamber. The conditions of this experiment were simulated by the in-house CFD code and results were promising when compared to experimental data. Details of the case chosen for comparison are summarized in Table 2.

Table 2 Experimental data conditions

Data Type	Quantity (unit)
Injection duration	1.5 (ms)
Fuel temperature	363 (K)
Injected mass	3.46 (mg)
Fuel type	n-Heptane
Ambient temperature	440 (K)
Ambient pressure	2.93 (MPa)
Nozzle diameter	0.084 (mm)

Figure 5 shows the calculated spray tip penetration and experimental data versus time. In the first stages of injection, there is an under-estimation in CFD results which is because of fully atomized assumption for the primary breakup and not taking into account the effect of liquid core and ligaments. But after this period of time, calculated results are in good agreement with experimental data. It should be mentioned that the standard modulation model is used for obtaining the results presented in Fig. 5.

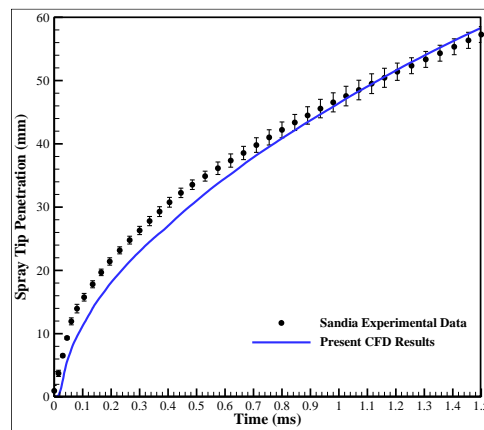


Fig. 5. Comparison between CFD results and experimental data of spray tip penetration.

### 3.3 Modulation Models

In this section, results of spray parameters like velocity profile, spray tip penetration, evaporation rate, and are shown with and without using two different classes of turbulence modulation models: standard, and consistent. All results are produced in moving mesh condition in which injection starts at CA=328 and finishes at CA=359.5 to provide 1.5 ms duration of injection according to experimental data (RPM=3500).

#### Velocity Profile

Figure 6 is the gas mixture radial velocity

distribution at the plane that separates cylinder region from piston bowl region at CA=350.

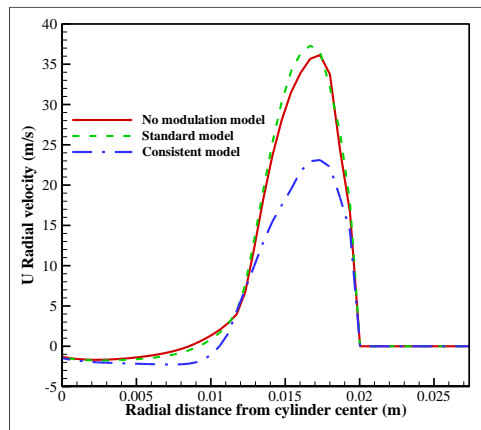


**Fig. 6. Radial velocity distribution comparison with different modulation models.**

It can clearly be seen that using consistent model reduces continuous phase velocity. This is due to the fact that this model transfers the kinetic energy of droplets to the gas mixture and this results in a reduction in droplets' velocity. So, droplets with lower velocity cannot accelerate the gas phase comparing to the one-way turbulence coupling.

On the other hand, when using the standard model, it can be seen clearly that just in some regions where a greater number of droplets exist, there is a shift in velocity profile. Again, the same reason stated in the previous paragraph but in an opposite manner can explain this behavior.

### Spray Tip Penetration

In order to assess the effect of the modulation models on spray characteristics, spray tip penetration diagram during injection is shown in Fig. 7.

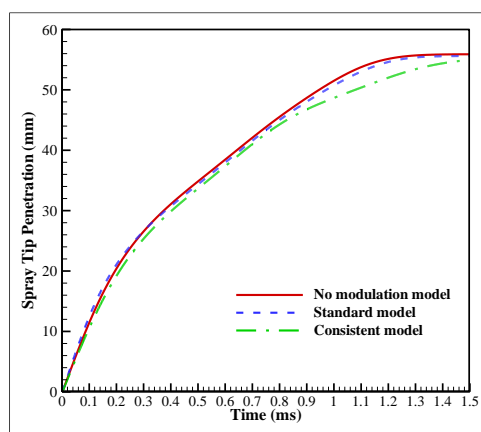


**Fig. 7. Spray tip penetration results by using different modulation models.**

Figure 7 shows that using modulation models has no major impact on predicting penetration. This can also be seen by looking at the spray structure at the end of the spray duration (Fig. 8).

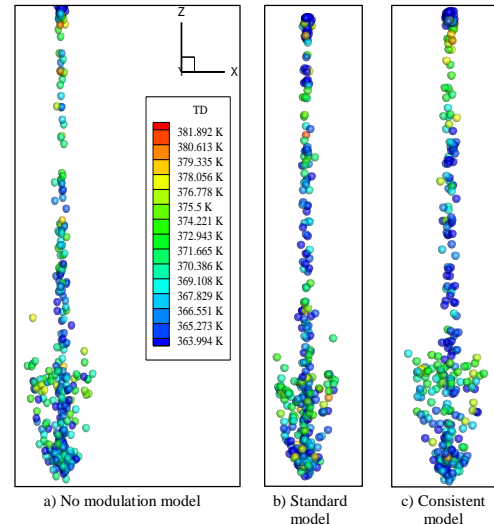


**Fig. 8. Spray structures using different modulation models.**

But it can be inferred that consistent model predicts a lower penetration which is due to higher turbulence in the field around particles and this resulted in a higher rate of evaporation. Evaporation rate diagrams can help us to find a proof for this conclusion.

### Evaporation Rate

Figure 9 is depicting the evaporation rate of droplets during injection time in which results of two different modulation models are compared with the results when no modulation model is considered.

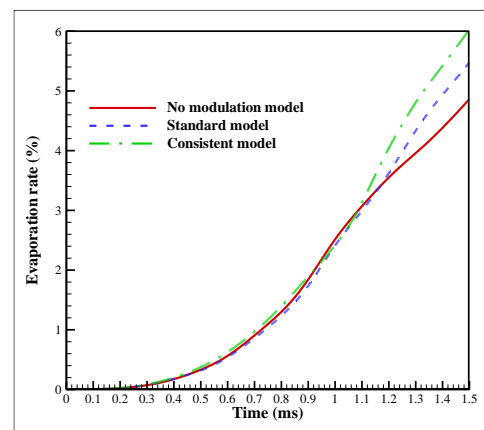


**Fig. 9. Evaporation rate vs. time comparison with different modulation models.**

In Fig. 9, both models are predicting higher rates of evaporation in comparison to no modulation model. This can be explained by the changes in flow field around particles that is higher turbulent kinetic energy when consistent model is used and higher velocity when standard model is employed. This also is apparent from a relatively more dispersed shape of spray at the end of spray duration in Fig. 8(c). Both factors are providing a condition which leads to a higher rate of evaporation but in consistent model, this increase is much more noticeable.

A higher rate of evaporation leads to having a smaller

droplet diameter. This can be seen in Fig. 10, in which the smallest mean diameter is predicted by the consistent modulation model which has a higher rate of evaporation.

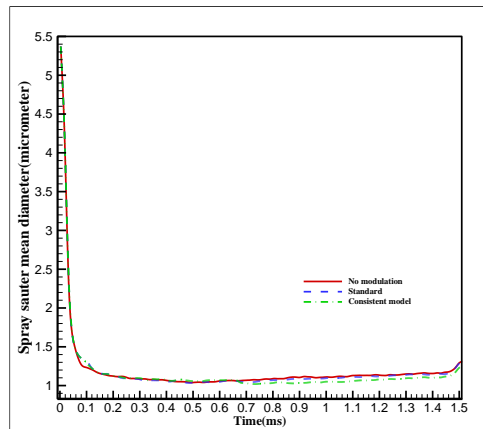


**Fig. 10. Spray Sauter mean diameter results by using different modulation models.**

#### Spray Mean Temperature

The variation of the mean temperature of droplets during spray injection time is shown in Fig. 11. It can be seen that the maximum mean temperature occurs in the early stages of injection. This is because of the droplet's heating up phenomenon. In the standard modulation model, because of the higher rate of evaporation and lower accessibility to high-temperature gas, the lower maximum temperature is predicted. Likely, in the consistent modulation model, a higher rate of evaporation leads to a lower prediction of maximum mean temperature, compared to no modulation model. On the latest stages of spray injection, there are slight differences among results obtained by modulation models.

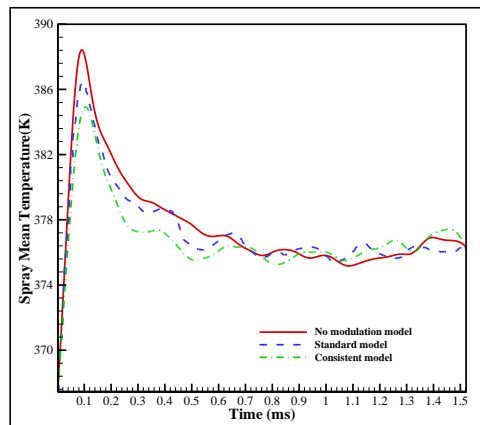


**Fig. 11. Spray mean temperature results by using different modulation models.**

#### 4. CONCLUSION

Results presented in the earlier section were on making a comparison between the one-way and two-way coupling of turbulence. First the influence of using different modulation models on the flow field

was investigated. Results showed that using the consistent type of models can alter the velocity profile to a high degree. The characteristic of this type of model is that it can predict a higher turbulence kinetic energy when droplets are injected. On the other hand, standard models can only predict a reduction in turbulence kinetic energy because of existing droplets. The change in the flow field and turbulence characteristics of continuous phase can also have some back-effects on the spray behavior. Results revealed that this change in the flow field can cause a much higher evaporation rate when consistent model is used. It can be inferred that using modulation models is of great importance in CFD simulation of evaporating sprays. Because predicting a more accurate flow field can result in a better prediction of spray characteristics. Also, more researches are needed on the proper model for using in CFD modeling of sprays under a wide range of working conditions. For example, in the flows with higher turbulence intensity. This can be used to suggest a more accurate tool for designing purposes and pollution predictions for internal combustion engines.

#### REFERENCES

- Ahmadi-Befrui, B., A. Gosman, R. Issa and A. Watkins (1990). EPISO—An implicit non-iterative solution procedure for the calculation of flows in reciprocating engine chambers. *Computer methods in applied mechanics and engineering* 79, 249-279.
- Alvandifar, N., M. Abkar, Z. Mansoori, M. S. Avval and G. Ahmadi (2011). Turbulence modulation for gas-particle flow in vertical tube and horizontal channel using four-way Eulerian-Lagrangian approach. *International Journal of Heat and Fluid Flow* 32, 826-833.
- Balachandar, S. and J. K. Eaton (2010). Turbulent dispersed multiphase flow. *Annual Review of Fluid Mechanics* 42, 111-133.
- Bilger, R. (1975). A note on Favre averaging in variable density flows. *Combustion Science and Technology* 11, 215-217.
- Borman, G. and J. H. Johnson (1962). Unsteady vaporization histories and trajectories of fuel drops injected into swirling air. *SAE Technical Paper* 0148-7191.
- Chen, C. and P. Wood (1985). A turbulence closure model for dilute gas - particle flows. *The Canadian journal of chemical engineering* 63, 349-360.
- Crowe, C. T. (2000). On models for turbulence modulation in fluid-particle flows. *International Journal of Multiphase Flow* 26, 719-727.
- Crowe, C. T. (2005). *Multiphase flow handbook* 59: CRC press.
- Ebrahimi, M. and M. Crapper (2017). CFD-DEM simulation of turbulence modulation in

- horizontal pneumatic conveying. *Particuology* 31, 15-24.
- Elghobashi, S. (1994). On predicting particle-laden turbulent flows. *Applied scientific research* 52, 309-329.
- Elghobashi, S. and T. Abou-Arab (1983). A two - equation turbulence model for two - phase flows. *The Physics of Fluids* 26, 931-938.
- Faeth, G. (1977). Current status of droplet and liquid combustion. *Progress in Energy and Combustion Science* 3, 191-224.
- Ferrante, A. and S. Elghobashi (2003). On the physical mechanisms of two-way coupling in particle-laden isotropic turbulence. *Physics of fluids* 15, 315-329.
- Gore, R. and C. T. Crowe (1989). Effect of particle size on modulating turbulent intensity. *International Journal of Multiphase Flow* 15, 279-285.
- Hetsroni, G. (1989). Particles-turbulence interaction. *International Journal of Multiphase Flow* 15, 735-746.
- Isbin, H. S. (1970). *One- dimensional two- phase flow*, Graham B. Wallis, McGraw- Huill, New York. *AICHE Journal*, 16(6), 896-1105.
- Khaleghi, H., D. Ganji and A. Omidvar (2008). Comparison of various droplet breakup models in gas-liquid flows in high pressure environments. *Iranian Journal of Science and Technology-Transaction B: Engineering* 32, 385-400.
- Lain, S. and M. Sommerfeld (2003). Turbulence modulation in dispersed two-phase flow laden with solids from a Lagrangian perspective. *International Journal of Heat and Fluid Flow* 24, 616-625.
- Lain, S. and M. Sommerfeld (2008). Euler/Lagrange computations of pneumatic conveying in a horizontal channel with different wall roughness. *Powder Technology* 184, 76-88.
- Lightstone, M. F. and S. M. Hodgson (2004). Turbulence Modulation in Gas - Particle Flows: A Comparison of Selected Models. *The Canadian Journal of Chemical Engineering* 82, 209-219.
- Lun, C. (2000). Numerical simulation of dilute turbulent gas-solid flows. *International Journal of Multiphase Flow* 26, 1707-1736.
- Luo, K., M. Luo and J. Fan (2016). On turbulence modulation by finite-size particles in dilute gas-solid internal flows. *Powder Technology* 301, 1259-1263.
- Meyer, D. W. (2012). Modelling of turbulence modulation in particle-or droplet-laden flows. *Journal of Fluid Mechanics* 706, 251-273.
- Paris, A. and J. Eaton (2001). *Turbulence attenuation in a particle-laden channel flow*. PhD Thesis. Mechanical Engineering Stanford University.
- Ranz, W. and W. Marshall (1952). Evaporation from drops. *Chemical Engineering Progress* 48, 141-146.
- Reitz, R. D. and R. Diwakar (1986). Effect of drop breakup on fuel sprays. *SAE Technical Paper* 0148-7191.
- Sandia, National Laboratories Engine Combustion Network (ECN). [Visited 2017 8 Nov]; Available from: <https://ecn.sandia.gov/ecn-data-search/>.
- Shuen, J. S., L. D. Chen and G. Faeth (1983). Evaluation of a stochastic model of particle dispersion in a turbulent round jet. *AICHE Journal* 29, 167-170.
- Watkins, A. and H. Khaleghi (1990). Modelling diesel spray evaporation using a noniterative implicit solution scheme. *Applied Mathematical Modelling* 14, 468-474.
- Yuu, S., N. Yasukouchi, Y. Hiroswawa and T. Jotaki (1978). Particle turbulent diffusion in a dust laden round jet. *AICHE Journal* 24, 509-519.